

## Effect of electropulsing rolling on mechanical properties and microstructure of AZ31 magnesium alloy

Chun XU, Ya-nan LI, Xiao-hua RAO

School of Materials Science and Engineering, Shanghai Institute of Technology, Shanghai 201418, China

Received 17 October 2013; accepted 14 November 2014

**Abstract:** Electropulsing rolling (ER) and warm rolling (WR) processes were performed to roll AZ31 magnesium alloy sheets. Mechanical properties, microstructure and texture evolution of these specimens were investigated after rolling. The results indicate that electropulsing accelerates the recrystallization of AZ31 alloy sheets during hot rolling. After electropulsing rolling at a relatively low temperature, the microstructure of the sample shows fine equiaxed recrystallized grains with a lower density of dislocations and precipitates. In contrast, the microstructure of the sample after warm rolling shows elongated grain, numerous deformed twins, and a high density of dislocation and precipitates. Electropulsing rolling helps weaken the basal fiber texture. Although both the alloy sheets (ER and WR) have typical basal fiber texture, the maximum pole intensity of basal in ER sample is weaker. ER sheet has higher yield strength and elongation compared to WR sheet. As a promising technique, electropulsing rolling can be used to improve the microstructure and mechanical properties of materials.

**Key words:** electropulsing; recrystallization; texture; AZ31 magnesium alloy

### 1 Introduction

Magnesium alloys are the lightest metallic structural materials. Compared with steels and aluminum alloys, they have higher specific strength and rigidity, therefore, they are the most attractive materials in applications of transportations and mobile electronics for reducing weight [1]. However, the use of magnesium in industry is limited because of its poor ductility at room temperature, due to its hexagonal closed-packed (HCP) crystal structure [2]. Although, according to some reports, the ductility of magnesium alloys could be improved by raising the rolling temperature (between 250 °C and 450 °C) to activate the non-basal slip systems [3–5], but the high temperature may also lead to thermal stress, warpage, and reduce tolerance control. Electropulsing has been applied for improving the plasticity of magnesium alloys [6–8] and controlling microstructure [9–12]. LIAO et al [8] indicated that electropulsing combined with warm rolling process tended to increase the elongation of AZ31 magnesium alloy strips. XU et al [9] found that the mechanism for increasing the elongation was mainly based on dynamic

recrystallization (DRX). LI et al [10] investigated the effect of electroplastic differential speed rolling (EDSR) on manufacturing thin AZ31 magnesium alloy strip. The results indicated that the ductility of rolled strip was significantly enhanced by EDSR. In the previous studies [6–12], the effects of rolling parameters of electropulsing rolling process or warm rolling process on the improvement of room ductility and deformability of magnesium alloys were studied. However, there are limited numbers of studies on the differences between microstructure, texture and mechanical properties of magnesium sheets in two rolling processes. In this work, electropulsing combined with conventional rolling process, named as electropulsing rolling process (ER), was applied to produce AZ31 magnesium alloy strips. The effects of warm rolling process (WR) and ER on the mechanical properties, texture and microstructure of magnesium alloy were studied and compared.

### 2 Experimental

A commercial AZ31B plate (Mg–3Al–1Zn, mass fraction, %) with 110 mm in width and 4 mm in thickness was used as the starting material in this work.

The warm rolling (WR) was carried out to achieve a sheet thickness of 0.7 mm. The samples were firstly pre-heated to 350 °C for 15 min to assure thorough heating. Between each pass, the samples were pre-heated for 2 min. At the same time, two rolls were heated so as to make their surface temperatures rise up to the demanded temperature of 250 °C. The rolling was performed with a reduction of approximately 20% per pass without lubrication. The warm rolling parameters are listed in Table 1. In comparison, electropulsing rolling (ER) was conducted under the above rolling schedule, but two rolls were not heated. The schematic view of electropulsing rolling process is shown in Fig. 1. Pulse currents were applied to the AZ31 magnesium alloy strip directly between the anode (upper roll) and the cathode (lower roll) when the strip was moved. The pulse power source was applied to discharge unidirectional pulses with frequency  $f=100$  Hz, peak current density  $J_m=5.7$  A/mm<sup>2</sup> and duty ratio  $D=80\%$ . The details are given in Table 1. All as-rolled sheets were subsequently cooled in air.

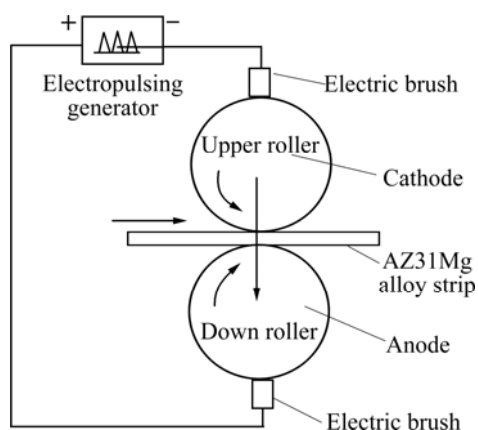


Fig. 1 Schematic view of ER process

The uniaxial tensile test was conducted at room temperature to measure the mechanical properties. Tensile samples of dog-bone geometry with 25 mm in gauge length, 10 mm in width and 50 mm in total length, were cut along plane coinciding with the rolling direction. Tensile test was carried out at room temperature at the rate of 0.5 mm/min with the tensile axis parallel to the rolling direction. Under each condition, five samples were measured.

Microstructure evolution of the rolled samples was also observed by optical microscopy (OM), electron

backscattering diffraction (EBSD) and transmission electron microscopy (TEM). The samples for optical observation were polished and etched with the solution of picric acid (6 g), acetic acid (20 mL), ethanol (50 mL) and distilled water (20 mL). The samples for EBSD orientation mapping were electrolytically polished. For TEM observation, the samples of 3 mm in diameter were ground, punched and then electropolished in an electrolyte of 500 mL methanol, 100 mL but-oxyetha-nol, 5.6 g magnesium perchlorate and 2.3 g lithium chloride by using a twin jet electropolishing equipment at  $-30$  °C and an applied voltage of 40 V.

### 3 Results

#### 3.1 Mechanical properties

The effects of WR and ER on mechanical properties of the samples are given in Table 2. The yield strength and elongation of the samples under ER are higher than those under WR. However, the tensile strength of the samples under ER is lower than that under WR.

Table 2 Mechanical properties of samples after warm rolling (WR) and electropulsing rolling (ER)

Process	Yield strength/ MPa	Tensile strength/ MPa	Elongation/ %
WR	181	271	16.5
ER	190	254	19.5

#### 3.2 Microstructure of samples

Figure 2 shows the microstructure of the as-received alloy and the samples after rolling. As can be seen in Fig. 2(a), the average grain size of the as-received sample of AZ31 strip is about 40  $\mu\text{m}$ . After electropulsing rolling (ER), there are small and equiaxed recrystallized grains with an average size of about 10  $\mu\text{m}$  in the microstructure, as shown in Fig. 2(b), which implies that DRX, as a softening mechanism [13], occurs during ER.

The microstructures of the sample after warm rolling are shown in Figs. 2(c) and 2(d), and Fig. 2(d) shows the high magnification of black rectangle in Fig. 2(c). It can be seen that grains are elongated slightly and numerous deformed twins are formed. Some elongated grains, especially some large grains (coarser than 30  $\mu\text{m}$ ) are surrounded by smaller recrystallized

Table 1 Rolling conditions for warm rolling (WR) and electropulsing rolling (ER)

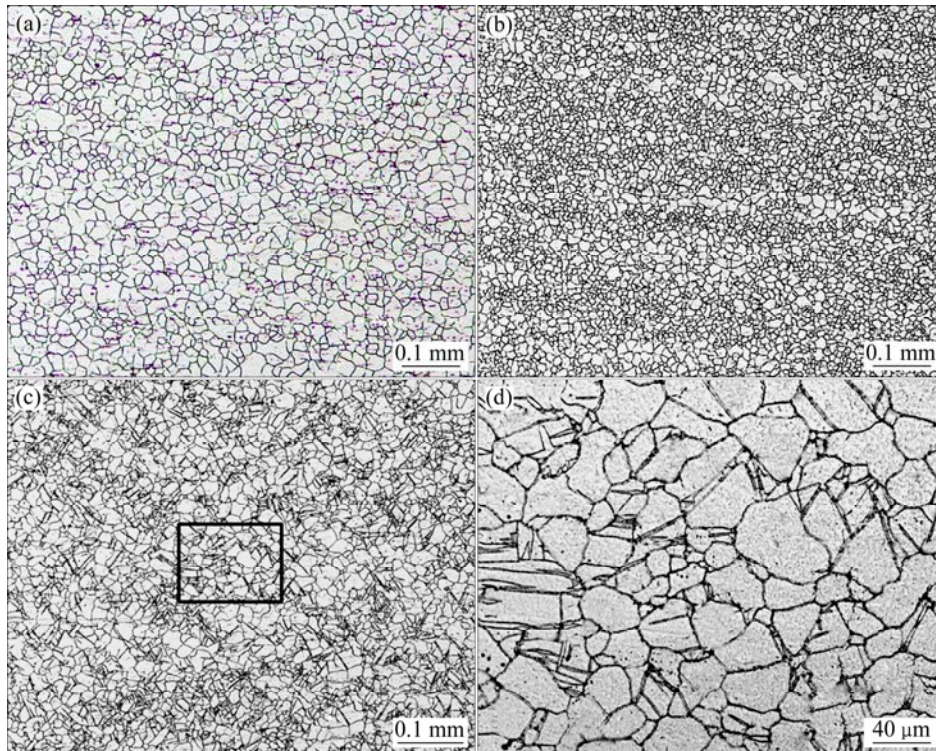
Process	Roller's surface temperature	Sample heating	Pulses current	Lubrication
WR	250 °C	350 °C for 2min	Not available	Unlubricated
ER	Room temperature	before each pass	$f=100$ Hz, $J_m=5.7$ A/mm <sup>2</sup> , $D=80\%$	Unlubricated

grains. Furthermore, some recrystallization nuclei form inside the twins and grow along the twin boundaries into strip-like grains, which give rise to the inhomogeneous microstructure. This means that the dominant deformation mechanism of the samples under WR is twinning.

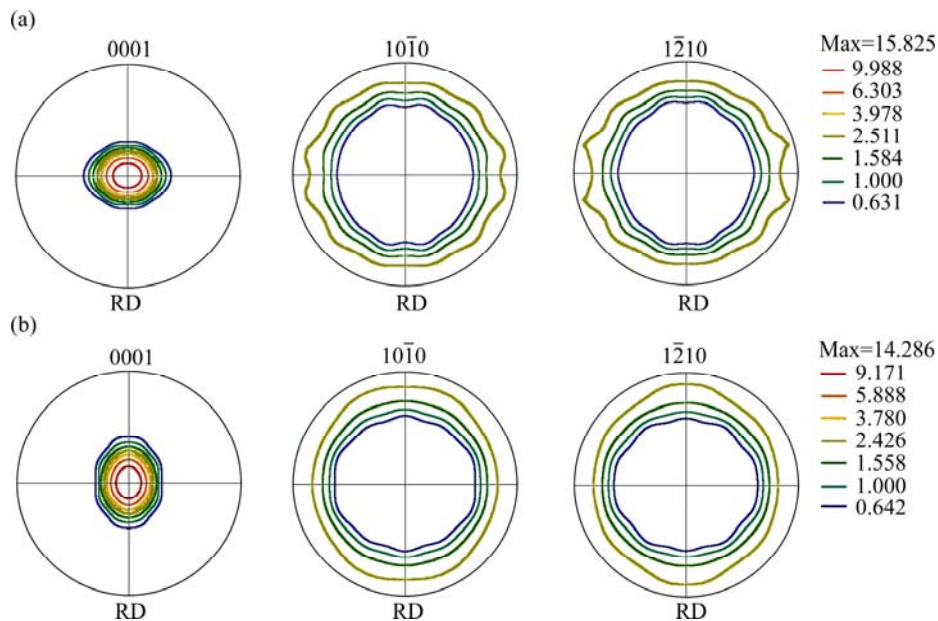
**3.3 Texture of samples**

Figure 3 shows the (0001), (10 $\bar{1}$ 0) and (1 $\bar{2}$ 10) pole figures of AZ31 Mg alloy sheets produced by warm

rolling (WR) and electropulsing rolling (ER). The maximum pole intensities of (0001) pole figures are 15.825 and 14.286 for the warm rolled sample and electropulsing rolled one, respectively. The major texture components of these samples can be expressed by ND//{0001} fiber texture. The texture of electropulsing rolled AZ31Mg alloy sheets shows typical basal fiber texture, while the warm rolled samples show that the basal pole tilts to transverse direction, as shown in Fig. 3(a).



**Fig. 2** Optical microstructures of raw sample (a), ER sample (b), and WR sample (c, d)



**Fig. 3** (0001), (10 $\bar{1}$ 0) and (1 $\bar{2}$ 10) pole figures of samples processed by (a) WR and (b) ER

Figure 4 shows the texture evolution of the WR and ER samples, with the Euler angle positions and Miller–Bravies indices of typical texture components in the orientation distribution function (ODF) presented in Fig. 4(c) for clarity. The dominant texture component of warm rolled sample is  $\{0001\}$  basal fiber texture. However, the characteristics of dominant deformation texture component for electropulsing rolled sample are tilted toward a position  $\sim 30^\circ$  away from the  $\{0001\}$  basal fiber texture. The maximum intensities of warm rolled sample and electropulsing rolled sample are 18.794 and 15.679, respectively. So the basal fiber texture of the

electropulsing rolled sample is obviously weakened.

The IPF+GB maps of the samples after being rolled are illustrated in Fig. 5, where the high angle boundaries (HAB) with misorientation larger than  $15^\circ$  are labeled by black bold line and the low angle boundaries (LAB) with misorientation within  $2\text{--}15^\circ$  are labeled by thin white line. Figure 6 shows the misorientation angle distribution of the EBSD samples based on Fig. 5. A large number of LAB and fragmented substructures mixed with many deformation twins appear in the primary grains of the warm-rolled (WR) sample, as shown in Fig. 5(a).

The results in Fig. 6(a) confirm that the warm rolled

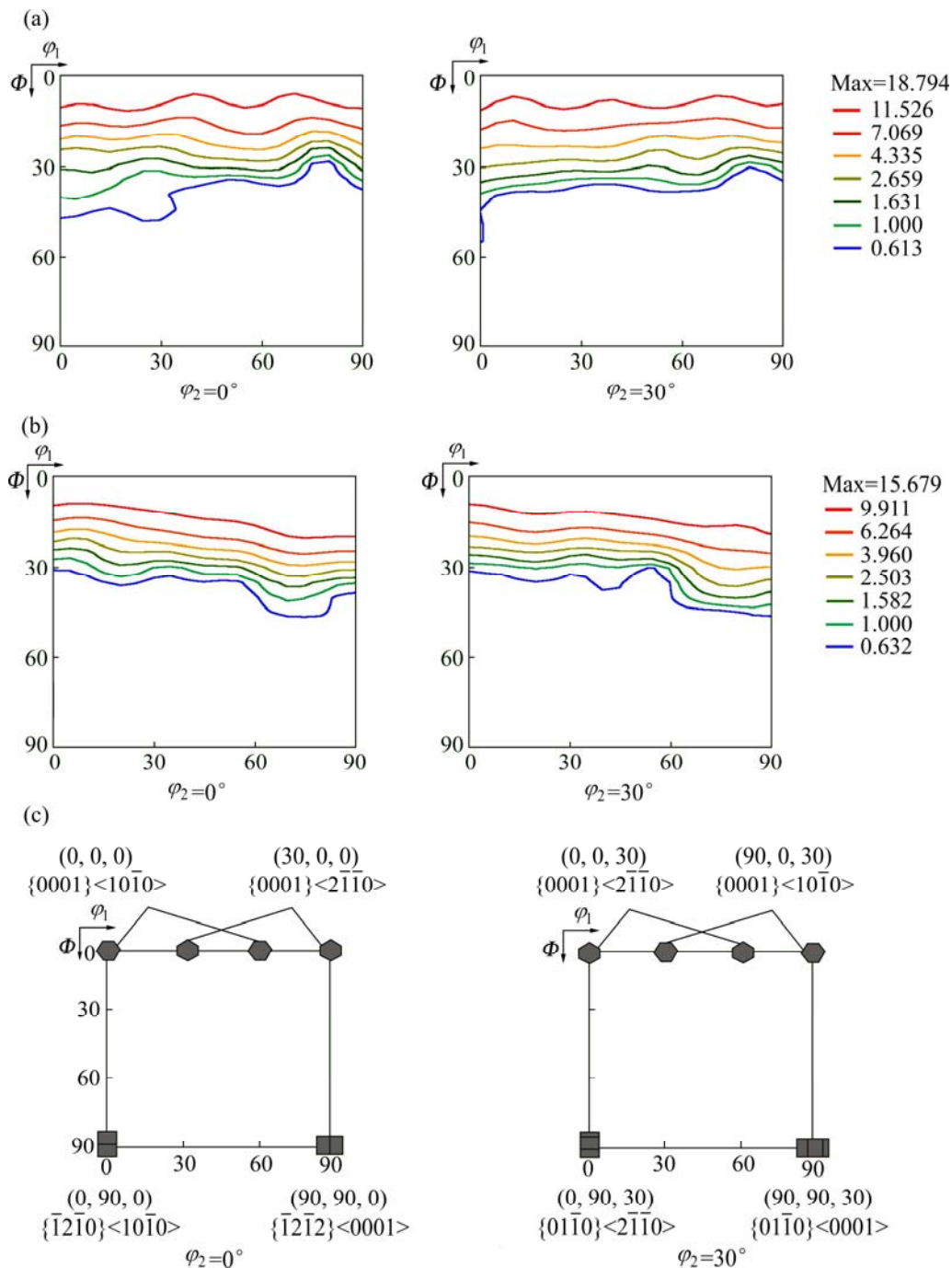


Fig. 4 Orientation distribution function (ODF) of samples: (a) WR; (b) ER; (c) Typical texture components in ODF

sample mainly consists of misorientation angle distribution peaks of  $2\text{--}10^\circ$ . However, the amount of the misorientation angle distribution of  $2\text{--}10^\circ$  in the electropulsing rolled sample decreases and a broad misorientation angle distribution in the range of  $15\text{--}60^\circ$  in electropulsing rolled sample becomes predominant, as shown in Fig. 6(b). It means that recrystallization is completed and all the primary grains are consumed by many fine recrystallized grains after being electropulsing rolled. So apparent grain growth occurs and relatively homogeneous microstructure of equiaxed grains is obtained, as shown in Fig. 2(b). Since the electropulsing rolled sample shows higher frequency of high angle boundary than that of the warm rolled sample, it indicates more random distribution of grain.

The distributions of grain size based on Fig. 5 are summarized in Fig. 7. It can be seen that the grain size is inhomogeneous in the two samples. But the microstructures of the electropulsing rolling sample are more uniform in shape than that of the warm rolling sample. After the ER, the grains are refined to be smaller than  $10\ \mu\text{m}$  compared to the grains after the WR.

### 3.4 Precipitates of samples

Figure 8 shows TEM micrographs for the warm rolled sample. The microstructure of warm rolled samples consists of equiaxed recrystallized grains, twins and precipitates, and some new sub-grains are developed. There is a high density of dislocations inside the subgrains, as shown in Fig. 8(a). Some regions of twins with sharp boundaries also occur in parallel bundles and encroach on each other laterally, as shown in Fig. 8(b). In these twins, many dislocations are visible, some distinctly on slip planes, and others in tangles. Most of the blocky-shaped precipitates over  $2\ \mu\text{m}$  in size are clustered in a narrow and long belt in the grains, which is shown in Fig. 8(c).

After pulse currents are applied to the conventional normal rolling process, there is a great difference among the TEM micrographs. The microstructure of ER samples is composed of finer equal axial recrystallized grains with a lower density of dislocations, as shown in Fig. 9. No twins are observed in the microstructure of ER samples. Similar to the microstructure of the warm rolled samples, blocky-shaped precipitates are scattered within the grains and dispersed in a long belt shape, too. TEM

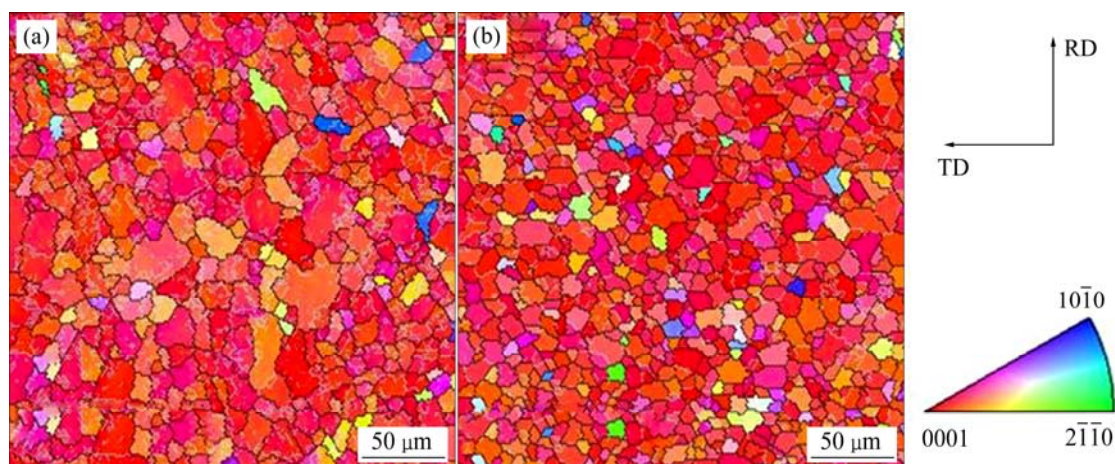


Fig. 5 IPF+GB maps of RD–TD plane for WR sample (a) and ER sample (b)

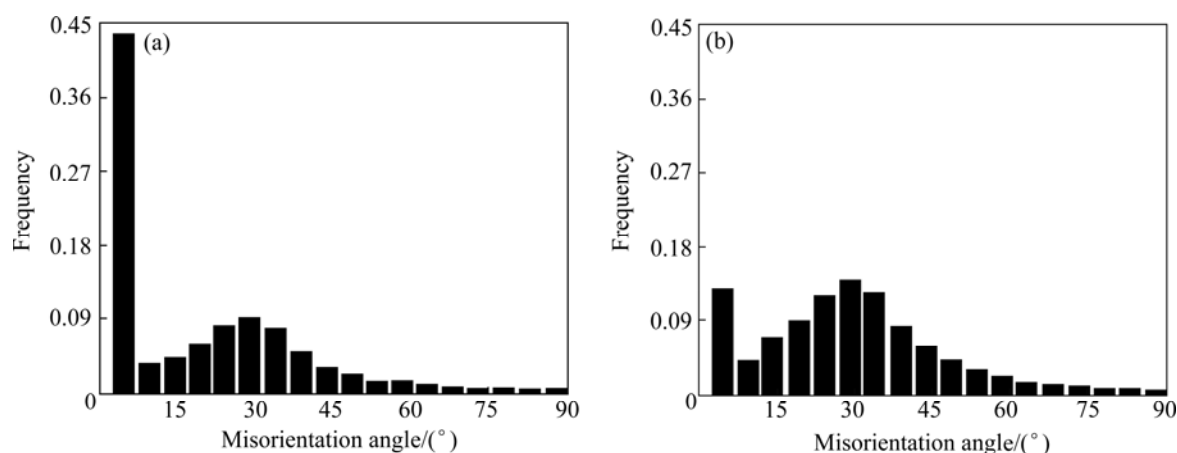
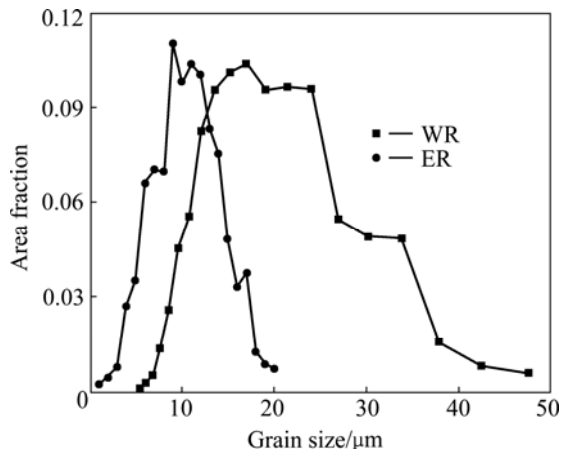
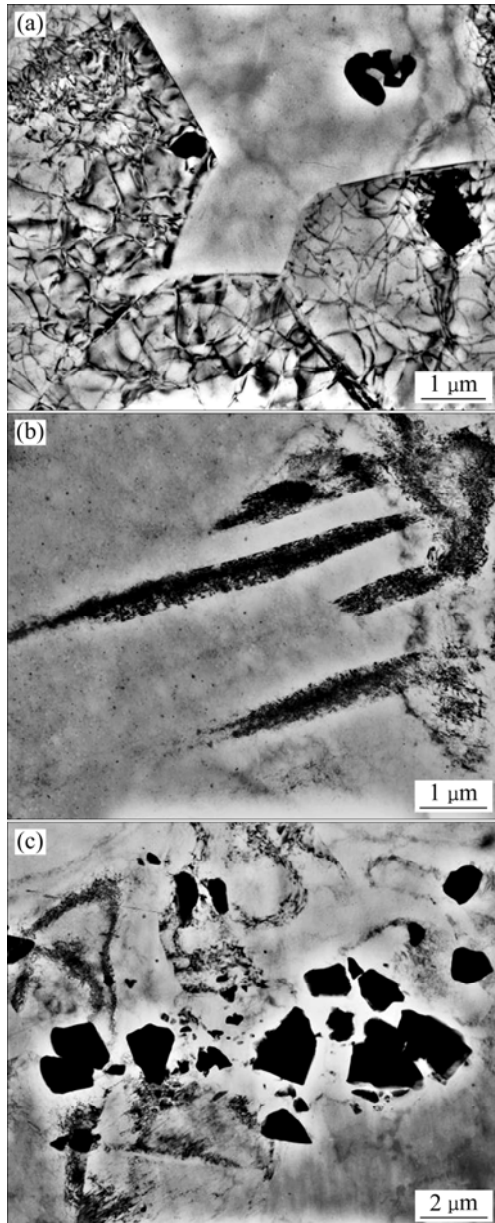


Fig. 6 Misorientation angle distribution of warm-rolled sample (a) and electropulsing rolled sample (b)



**Fig. 7** Grain size distribution of rolled samples



**Fig. 8** TEM microstructures of WR sample: (a) Subgrains; (b) Twins; (c) Precipitates

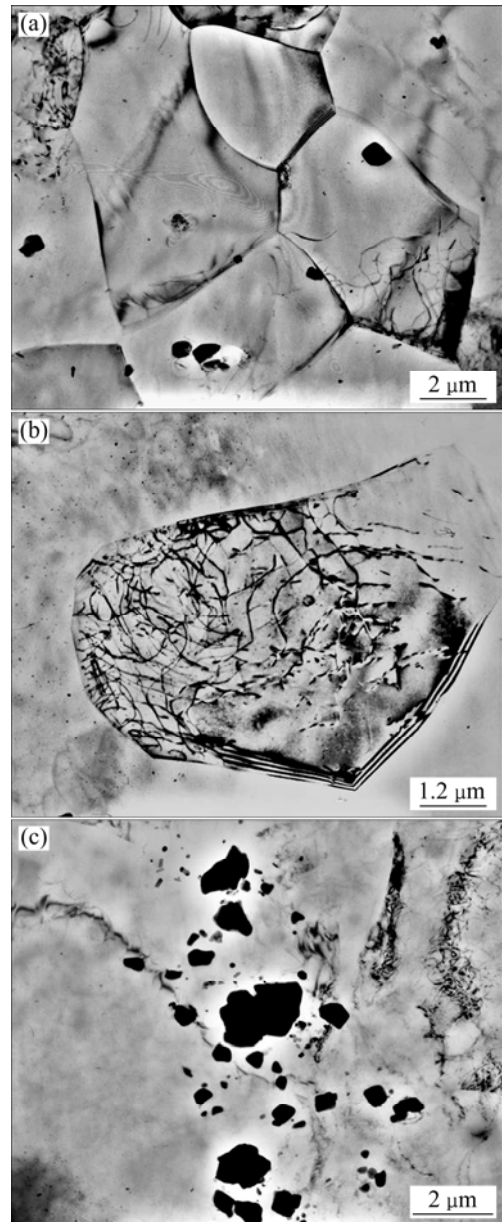


**Fig. 9** TEM microstructures of ER sample: (a) Equiaxed recrystallized grains; (b) Subgrain; (c) Precipitates

images show that the precipitates in WR and ER samples are  $Mg_{17}Al_{12}$ , as shown in Figs. 10 and 11.

#### 4 Discussion

Warm rolling tests are carried out at the warm rolls with the surface temperature of 250 °C, and the actual deforming temperature of warm rolled samples would exceed 250 °C. As a consequence of the high critical stresses required for the activation of non-basal slip systems, dynamic recrystallization plays a vital role in the deformation of magnesium, particularly at a deformation temperature of 200 °C [13,14]. From the OM and TEM images of warm rolled samples, a lot of

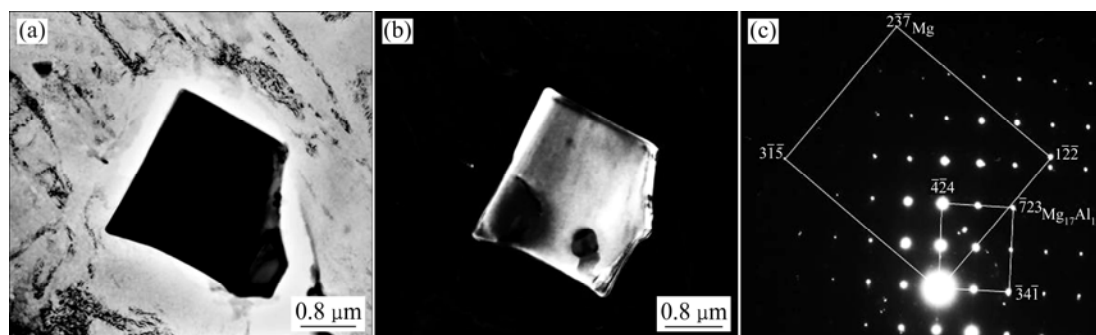


**Fig. 10** TEM images of  $Mg_{17}Al_{12}$  precipitate in WR sample: (a) Bright field; (b) Dark field; (c) Diffraction pattern of  $Mg_{17}Al_{12}$

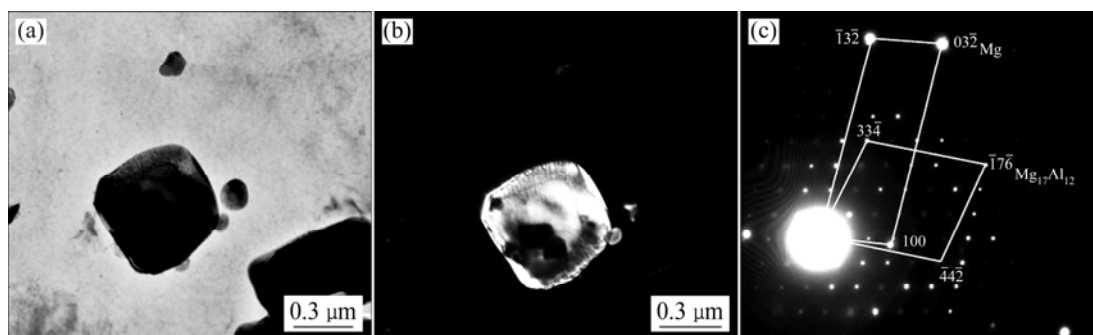


**Fig. 11** TEM images of  $Mg_{17}Al_{12}$  precipitate in ER sample: (a) Bright field; (b) Dark field; (c) Diffraction pattern of  $Mg_{17}Al_{12}$

dynamic recrystallized grains are observed, especially some recrystallization nuclei form inside the twins and grow along the twin boundaries into strip-like grains. And characteristic thin twins could still be clearly distinguished. It is thus reasonable to conclude that partial dynamic recrystallization occurs in the microstructure of warm rolled samples.

Although electropulsing rolling tests are also carried out under conventional normal rolling conditions, and pulse current is also applied to the above rolls. With the aid of electropulsing, the number of piling-up dislocations decreases and the number of mobile dislocations increases. Therefore, the densities of dislocations could be in good balance between grain boundary and inside the grain even at a low temperature [15,16]. That is the reason why finer equal axial recrystallized grains without twins are observed in OM and TEM micrographs of the electropulsing rolled sample (Fig. 2(b) and Fig. 9). This indicates that microstructures are totally dynamically recrystallized at electropulsing rolling conditions. In EBSD images (Figs. 5 and 7), the average grain size of the electropulsing rolled sample is obviously finer than that of the warm rolling sample. Furthermore, the basal fiber texture is obviously weakened and the texture is tilted toward a position  $\sim 30^\circ$  away from the (0001) poles (Fig. 4). Besides, the electropulsing rolled sample shows higher frequency of high angle boundary than the warm rolled sample (Fig. 6), which indicates more random distribution of grains. Some researcher have reported that

the ductility enhancement is associated with the slight change in the basal texture [15] and/or reduction in grain size [14]. As a result, the electropulsing rolled sample owns little lower tensile strength and significantly higher elongation compared with that of the warm rolled sample.

## 5 Conclusions

1) Electropulsing tremendously accelerates the recrystallization behavior of AZ31 alloy sheet. Recrystallization would finish when electropulsing rolling at a relatively low temperature, and the microstructure shows fine recrystallized grains with a lower density of dislocations and precipitates. In contrast, the microstructure of the sample after warm rolling shows elongated grain, numerous deformed twins, and a high density of dislocation and precipitates.

2) Electropulsing rolling helps to weaken the basal fiber texture. Although both the alloy sheets (ER and WR) have typical basal fiber texture, the maximum pole intensity of basal in ER sample is weaker.

3) ER sheet has higher yield strength and elongation compared to the WR sheet. Electropulsing rolling can be used to improve the microstructure and mechanical properties of magnesium alloys.

## References

- [1] DING W J, JIN L, WU W X, DONG J. Texture and texture

- optimization of wrought Mg alloy [J]. The Chinese Journal of Nonferrous Metals, 2011, 21: 2371–2381. (in Chinese)
- [2] XIA W J, CAI J G, CHEN Z H, CHEN G, JIANG J F. Microstructure and room temperature formability of AZ31 magnesium alloy produced by differential speed rolling [J]. The Chinese Journal of Nonferrous Metals, 2010, 20: 1247–1253. (in Chinese)
- [3] HUANG G S, ZHANG H, GAO X Y, SONG B, ZHANG L. Forming limit of textured AZ31B magnesium alloy sheet at different temperatures [J]. Transactions of Nonferrous Metals Society of China, 2011, 21: 836–843.
- [4] LIU J W, CHEN Z H, CHEN D, LI G F. Deformation mechanism and softening effect of extruded AZ31 magnesium alloy sheet at moderate temperatures [J]. Transactions of Nonferrous Metals Society of China, 2012, 22: 1329–1335.
- [5] MAKSOU D I A, AHMED H, RODEL J. Investigation of the effect of strain rate and temperature on the deformability and microstructure evolution of AZ31 magnesium alloy [J]. Materials Science and Engineering A, 2009, 504(1–2): 40–48
- [6] KIM D G, LEE K M, LEE J S, YOON Y O, SON Y T. Evolution of microstructures and textures in magnesium AZ31 alloys deformed by normal and cross-roll rolling [J]. Materials Letters, 2012, 75: 122–125.
- [7] JIANG Y B, TANG G Y, SHEK C H, LIU W. Microstructure and texture evolution of the cold-rolled AZ91 magnesium alloy strip under electropulsing treatment [J]. Journal of Alloys and Compounds, 2011, 509: 4308–4313.
- [8] LIAO H M, TANG G Y, JIANG Y B, XU Q, SUN S D, LIU J A. Effect of thermo-electropulsing rolling on mechanical properties and microstructure of AZ31 magnesium alloy [J]. Materials Science and Engineering A, 2011, 529: 138–142.
- [9] XU Q, GUAN L, JIANG Y B, TANG G Y, WANG S N. Improved plasticity of Mg–Al–Zn alloy by electropulsing tension [J]. Materials Letters, 2010, 64: 1085–1087
- [10] LI X P, WANG F, LI X H, TANG G Y, ZHU J. Improvement of formability of Mg–3Al–1Zn alloy strip by electroplastic differential speed rolling [J]. Materials Science and Engineering A, 2014, 618: 500–504
- [11] JIANG Y B, TANG G Y, SHEK C H, XIE J X, XU Z H, ZHANG Z H. Mechanism of electropulsing induced recrystallization in a cold-rolled Mg–9Al–1Zn alloy [J]. Journal of Alloys and Compounds, 2012, 536: 94–105.
- [12] XU Z H, TANG G Y, TIAN S Q, DING F, TIAN H Y. Research of electroplastic rolling of AZ31 Mg alloy strip [J]. Journal of Materials Processing Technology, 2007, 182: 128–133.
- [13] AL-SAMMAN T, GOTTSTEIN G. Dynamic recrystallization during high temperature deformation of magnesium [J]. Materials Science and Engineering A, 2008, 490(1–2): 411–420.
- [14] AGNEW S R, DUYGULU Ö. Plastic anisotropy and the role of non-basal slip in magnesium alloy AZ31B [J]. International Journal of Plasticity, 2005, 21(6): 1161–1193.
- [15] WATANABE H, MUKAI T, ISHIKAWA K. Differential speed rolling of an AZ31 magnesium alloy and the mechanical properties [J]. Journal of Material Science, 2004, 39(4): 1477–1480.
- [16] KUBOTA K, MABUCHI M, HIGASHI K. Processing and mechanical properties of fine-grained magnesium alloys [J]. Journal of Material Science, 1999, 34(10): 2255–2262.

## 脉冲电流轧制对 AZ31 镁合金微观组织与力学性能的影响

徐 春, 李亚楠, 饶晓华

上海应用技术学院 材料科学与工程系, 上海 201418

**摘 要:** 对比研究脉冲电流轧制工艺与温轧工艺对 AZ31 镁合金板材的力学性能、织构、微观组织与沉淀相等方面的影响。结果表明: 脉冲电流具有促进冷轧 AZ31 镁合金低温再结晶能力的作用。脉冲电流轧制后的镁合金板材组织由细小的等轴再结晶粒与析出相构成, 没有发现孪晶组织, 并且完全再结晶, 原始晶粒均被细小的再结晶晶粒取代, 再结晶晶粒内的位错密度低。而温轧镁合金组织则由稍拉长变形孪晶、粗大的再结晶晶粒和析出相构成, 再结晶的晶粒内位错密度高。两种轧制方式下的镁合金析出相均为  $Mg_{17}Al_{12}$ 。脉冲电流轧制后镁合金的组织具有典型基面织构的特征, 而脉冲电流轧制镁合金的组织则出现横向偏转; 脉冲电流轧制后镁合金的屈服强度与伸长率均比温轧镁合金的大, 但抗拉强度正好相反。

**关键词:** 脉冲电流; 再结晶; 织构; AZ31 镁合金

(Edited by Yun-bin HE)